Time is of the essence - investigating kinetic interactions between drug, endogenous neuropeptides and receptor

Nederpelt, I.

Chapter 3

Characterization of 12 GnRH peptide agonists – a kinetic perspective

Indira Nederpelt

Victoria Schuldt

Felix Schiele

Katrin Nowak-Reppel

Amaury E. Fernández-Montalván

Adriaan P. IJzerman

Laura H. Heitman

Adapted from *British Journal of Pharmacology* **2016** *173 (1): 128-41*

Abstract

Drug-target residence time is an important, yet often overlooked, parameter in drug discovery. Multiple studies have proposed an increased residence time to be beneficial for improved drug efficacy and/or longer duration of action.

Currently there are many drugs on the market targeting the gonadotropin-releasing hormone (GnRH) receptor for the treatment of hormone-dependent diseases. Surprisingly, the kinetic receptor binding parameters of these analogues have not yet been reported. Therefore, this project focused on determining the receptor binding kinetics of twelve GnRH peptide agonists, including many marketed drugs.

We successfully developed and optimized a novel radioligand binding competition association assay for the human GnRH receptor with the use of a radiolabeled peptide agonist, ^{125}I-triptorelin. In addition to radioligand binding studies, a homogenous time-resolved fluorescence (TR-FRET) Tag-lite™ method was developed as an alternative assay for the same purpose. Both assays were applied to determine the kinetic receptor binding characteristics of twelve high affinity GnRH peptide agonists. Results obtained from both methods were highly correlated. Interestingly, the binding kinetics of the peptide agonists were more divergent than their affinities with residence times ranging from 5.6 min (goserelin) to 125 min (deslorelin).

Our research provides new insights by incorporating kinetic, next to equilibrium, binding parameters in current research and development that can potentially improve future drug discovery targeting the GnRH receptor.

Introduction

Drug target residence time is emerging as an important parameter in the drug discovery process. Multiple studies provide evidence that the binding kinetics of drug target interactions rather than the typical equilibrium binding parameters are important for *in vivo* efficacy [1-4]. Several marketed drugs in the field of G protein-coupled receptors (GPCRs) have *retrospectively* been shown to display slow receptor dissociation rates, or, in other words, long receptor residence times [5]. For instance, the histamine H_1 receptor antagonist desloratidine was found to have a long residence time, which could explain its high potency and 24 hours duration of action observed in clinical studies [6]. Another example is the insurmountable antagonist for the angiotensin II subtype-1 (AT_1) receptor, telmisartan. The authors deemed the insurmountability and therefore improved efficacy of telmisartan to be partly due to its very slow dissociation from AT_1 receptors [7].

The hypothalamic neuropeptide gonadotropin-releasing hormone (GnRH) is a central mediator of reproductive functions. This decapeptide binds to a class A GPCR, namely the GnRH receptor (GnRHR) located mainly on pituitary gonadotrophs. Along with the pituitary, GnRH receptors are expressed in reproductive tissues, both normal and malignant, such as those of the prostate and mammary gland [8-11]. Upon receptor activation, the gonadotropins luteinizing hormone (LH) and follicle stimulating hormone (FSH) are synthesized and secreted from gonadotrophic cells. LH and FSH consecutively induce follicle stimulation and ovulation in females and promote steroidogenesis in both males and females [12].

The pulsatile release of GnRH from the hypothalamus is essential for the maintenance of ovarian function. Sustained exposure of GnRHR to GnRH or GnRH analogues leads to activation, commonly named ''flare'', followed by desensitization of GnRHR-mediated gonadotropin secretion. Accordingly, blockade by antagonists or desensitization of GnRHR-mediated gonadotropin secretion both ultimately reduce circulating levels of gonadotropins and gonadal steroids [13, 14]. This so called chemical castration underlies the therapeutic use of GnRH analogues to treat sex hormone-dependent diseases [15-17].

Consequently, considerable efforts have been put towards the development of agonists and antagonists targeting the GnRH receptor [18-22]. Only a few studies have examined the receptor binding kinetics of GnRH ligands. A paper of Heise *et al.* [23] described a scintillation proximity assay to qualitatively distinguish between fast and slowly dissociating antagonists for the GnRH receptor. The authors demonstrated that slow dissociation rates were responsible for large discrepancies between a ligand's K_i value determined at 30 minutes versus 10 hours and they suggested using the K_i ratio as a

screening method to select slowly dissociating compounds. Two other studies focused on a quantitative determination of receptor binding kinetics of small molecule GnRH antagonists. Here, a direct correlation between the insurmountability and slow dissociation rates of these antagonists was shown [24, 25].

Currently multiple peptide GnRH analogues have been approved for the treatment of advanced prostatic cancer, endometriosis, *in vitro* fertilization and more [15-17, 26-29]. Remarkably, the receptor binding kinetics of peptide GnRH receptor ligands have never been reported. Therefore, we developed a novel radioligand binding competition association assay that allowed us to determine the kinetic binding parameters and focused on twelve GnRH peptide agonists, including many marketed drugs (Table 1). In addition, we compared these kinetic parameters with those from a newly developed homogenous time-resolved fluorescent (HTRF) assay. Both assays may improve future drug discovery targeting the GnRH receptor by incorporating kinetic receptor binding parameters into current research and development trajectories.

Material & methods

Reagents and peptides

Deslorelin and fertirelin (Table 1) were obtained from Genway Biotech Inc. (San Diego, CA, U.S.A.) and American Peptide Company (Sunnyvale, CA), respectively. All other peptide analogs (Table 1) and bovine serum albumin (BSA) were purchased from Sigma-Aldrich Chemie B.V. (Zwijndrecht, The Netherlands). BCA (bicinchoninic acid) protein assay reagent was obtained from Pierce Chemical Company (Rockford, IL, U.S.A.). ^{125}I-triptorelin (specific activity 2200 Ci/mmol) was purchased from PerkinElmer (Groningen, The Netherlands). Chinese Hamster Ovary cells stably expressing the human gonadotropin-releasing hormone receptor (from now on CHOhGnRH cells) were kindly provided by MSD (Oss, The Netherlands). Tag-lite™ HEK293 cells containing a stably overexpressed human GnRH receptor labeled with Tb (from now on Tag-lite™ GnRH cells) were obtained as frozen stocks from Cisbio (Codolet, France). A buserelin-derived tracer, labeled at the ^{6th} position with a red emitting fluorophore and Tag-lite™-buffer (TLB) were also purchased from Cisbio (Codolet, France). All other chemicals and cell culture materials were obtained from standard commercial sources. The molecular target nomenclature (GnRHR) conforms to 'The Concise Guide to PHARMACOLOGY 2013/14: G Protein-Coupled Receptors' [30].

Cell Culture

For radioligand binding assays, CHOhGnRH cells were grown in Ham's F12/DMEM (1:1) medium supplemented with 10% normal bovine serum, 2 mM glutamine, penicillin (100 IU/mL), streptomycin (100 µg mL^{-1}) and G418 (200 µg mL^{-1}) at 37 °C in 5% CO_2.

For TR-FRET experiments, 1 ml (7 *10^6 cells ml^{-1}) of Tag-lite™ GnRH cells were thawed, washed with 15 ml ice-cold TLB, resuspended in 5 ml TLB and immediately used.

Membrane Preparation

CHOhGnRH cells were scraped from the plates in 5 mL PBS, collected and centrifuged at 700 *g* (3000 rpm) for 5 min. Derived pellets were pooled and resuspended in 50 mM Tris HCl buffer pH 7.4 at 25 °C supplemented with 2 mM $MgCl_2$, and subsequently homogenized with an UltraThurrax (Heidolph Instruments, Germany). The cytosolic fraction and membranes were separated by centrifugation at 100 000 *g* (31 000 rpm) in an Optima LE-80K ultracentrifuge (Beckman Coulter, Fullterton, CA, U.S.A.) for 20 min. at 4 °C. The pellet was resuspended and centrifugation was repeated. The obtained pellet was resuspended, membranes were aliquoted and stored at -80 °C. Membrane protein concentrations were determined using the BCA method with BSA as a standard [31].

Table 1: Amino acid sequences of the twelve examined GnRH peptide agonists. The differences between the peptides are expressed in bold.

	1	2	3	4	5	6	7	8	9	10
GnRH	pGlu*	His	Trp	Ser	Tyr	**Gly**	Leu	Arg	Pro	**Gly-NH_2**
Triptorelin	pGlu*	His	Trp	Ser	Tyr	**D-Trp**	Leu	Arg	Pro	**Gly-NH_2**
[D-Ala^6]-GnRH	pGlu*	His	Trp	Ser	Tyr	**D-Ala**	Leu	Arg	Pro	**Gly-NH_2**
[D-Lys^6]-GnRH	pGlu*	His	Trp	Ser	Tyr	**D-Lys**	Leu	Arg	Pro	**Gly-NH_2**
Fertirelin	pGlu*	His	Trp	Ser	Tyr	**Gly**	Leu	Arg	Pro	**NHEt***
Alarelin	pGlu*	His	Trp	Ser	Tyr	**D-Ala**	Leu	Arg	Pro	**NHEt***
Deslorelin	pGlu*	His	Trp	Ser	Tyr	**D-Trp**	Leu	Arg	Pro	**NHEt***
Leuprorelin	pGlu*	His	Trp	Ser	Tyr	**D-Leu**	Leu	Arg	Pro	**NHEt***
Nafarelin	pGlu*	His	Trp	Ser	Tyr	**D2Nal**	Leu	Arg	Pro	**Gly-NH_2**
Buserelin	pGlu*	His	Trp	Ser	Tyr	**Ser-tBu***	Leu	Arg	Pro	**NHEt***
Goserelin	pGlu*	His	Trp	Ser	Tyr	**Ser-tBu***	Leu	Arg	Pro	**aGly-NH_2***
Histerelin	pGlu*	His	Trp	Ser	Tyr	**His(Bzl)***	Leu	Arg	Pro	**NHEt***

*pGlu = pyroglutamic acid, D2Nal = (2-naphthyl)-D-alanine, Ser-tBu = serine-tert-butyl, His(Bzl) = N-benzyl-L-histidine, aGly-NH_2 = aza-glycine amine, NHEt = ethylamide

Radioligand Equilibrium Assays

Displacement experiments were performed as previously reported [32]. In short, membrane aliquots containing 15-20 µg protein were incubated in a total volume of 100 µL assay buffer (25 mM Tris HCl, pH 7.4 at 25 °C, supplemented with 2 mM $MgCl_2$, 0.1 % (w/v) BSA) at 25 °C for 2 hours. Ten concentrations of competing ligand were used in the presence of 30.000 cpm (~0.1 nM) ^{125}I-triptorelin. At this concentration, total radioligand binding did not exceed 10% of that added to prevent ligand depletion. Non-specific binding was determined in the presence of an excess amount of GnRH (1 µM). The reaction was terminated by the addition of 1 mL ice-cold wash buffer (25 mM Tris HCl, pH 7.4 at 25 °C, supplemented with 2 mM $MgCl_2$ and 0.05% (w/v) BSA). Separation of bound from free radioligand was performed by rapid filtration through Whatman GF/B filters saturated with 0.25% polyethylene imine (PEI) using a Brandel harvester. Filters were subsequently washed three times with 2 mL ice-cold wash buffer. Filter bound radioactivity was determined using a γ-counter (Wizard 1470, PerkinElmer).

Radioligand Kinetic Association and Dissociation Assays

Association experiments were carried out by incubating membrane aliquots containing 15-20 µg protein in a total volume of 100 µL assay buffer at 25 °C with 30.000 cpm (~0.1 nM) ^{125}I-triptorelin. The amount of radioligand bound to the receptor was determined at different time intervals for a total incubation time of 120 min.

Dissociation experiments were performed by preincubating membrane aliquots containing 15-20 µg protein in a total volume of 100 µL assay buffer at 25 °C for 45 min with 30.000 cpm (~0.1 nM) ^{125}I-triptorelin. After preincubation, dissociation was initiated by addition of an excess amount of GnRH (1 µM) in a total volume of 2.5 µL. The amount of radioligand still bound to the receptor was measured at various time intervals for a total incubation time of 120 min. The reaction was stopped and samples were harvested as described under *Radioligand Equilibrium Assays*.

Radioligand Kinetic Competition Association Assays

The binding kinetics of unlabeled ligands were quantified using the competition association assay based on the method by Motulsky and Mahan [33]. During optimization, three different concentrations of unlabeled triptorelin were tested; 0.3-, 1- and 3-fold its K_i value. The kinetic parameters of all other unlabeled ligands were determined at a concentration of 1-fold their K_i, unless stated otherwise. The competition association assay was initiated by adding membrane aliquots containing 15-20 µg protein in a total volume of 100 µL assay buffer at 25 °C with 50.000 cpm (~0.15 nM) ^{125}I-triptorelin in the absence or

presence of competing ligand. Of note, total radioligand binding did not exceed 10% of that added at this concentration to prevent ligand depletion. The amount of radioligand bound to the receptor was determined at different time intervals for a total incubation time of 120 min. The reaction was stopped and samples were harvested as described under *Radioligand Equilibrium Assays*.

TR-FRET Probe Equilibrium Assays

Unless otherwise specified, TR-FRET measurements were carried out using the conditions described in [34]. To determine the equilibrium affinity of the fluorescent probe, 5 µl Tag-lite™ GnRH cells (1400 cells μl^{-1}) were incubated for 1 h, to ensure signal stability, with increasing probe concentrations (ranging from 0 to 100 nM: Supplementary Figure S1) in a final volume of 10 µl. In parallel, a non-specific binding control was carried out in the presence of an excess amount of buserelin (100 µM). Binding signals were measured in a PHERAstar FS plate reader by exciting the Tb donor with 5 laser flashes at a wavelength of 337 nm and recording acceptor and donor emission fluorescence channels (A and B channels), at wavelengths of 520 nm and 490 nm respectively.

TR-FRET Equilibrium Probe Competition Assays

"Ready-to-use" assay plates containing serial dilutions of the test agonists were prepared as described in [34]. Subsequently 5 µl Tag-lite™ GnRH cells (1400 cells μl^{-1}) and 50 nM probe were added to the competitors and incubated at room temperature for 1 h, to ensure signal stability, in a final volume of 10 µl. Non-specific binding ("low signal") controls contained an excess amount of buserelin (100 µM), whereas in "high signal" controls, the test compounds were replaced by DMSO. Binding signals were recorded as described under *TR-FRET Probe Equilibrium Assays*.

TR-FRET Kinetic Probe Association and Dissociation Assays

Measurements were carried out in quadruplicate and in a final volume of 15 µl $well^{-1}$. First, a 5-point, 2-fold serial dilution of fluorescent probe (Supplementary Figure 2) was pre-dispensed on black 384 well low volume plates (Greiner) and the the PHERAstar FS injection system's syringes (previously washed with $NaOH/H_2O$) were either primed with 1500 µl solution of Tag-lite™ GnRH cells, (1000 cells μl^{-1}) or with 200 µM buserelin. Then, 4 µl of cells were quickly added to the probe with the first syringe and the association traces were recorded as described under *TR-FRET Probe Equilibrium Assays*, with kinetic intervals of 26 seconds. After 30 min, fluorescent probe dissociation was initiated by addition of 5 µl of an excess of unlabeled buserelin (final concentration 67 µM) with the second syringe and the

traces were recorded with kinetic intervals of 300 seconds in the same fashion. Alternatively a 1-point measurement was performed with 5 µL of probe (final concentration 25 nM) and 5 µL of Tag-lite™ GnRH cells (1400 cells/µL) and association was recorded with kinetic intervals of 120 seconds. After 24 min dissociation was initiated and recorded with the same kinetic interval.

TR-FRET Kinetic Probe Titration Assays

First, 5 µL of increasing concentrations of fluorescent probe was dispensed into 384 well plates, the injection system of the PHERAstar FS plate reader was primed with Tag-lite™ GnRH cells as described under *TR-FRET Probe Equilibrium Assays*. Then, 5 µl of cell solution was added with the syringe and the TR-FRET signals corresponding to probe association were recorded as described under *TR-FRET Probe Equilibrium Assays*.

TR-FRET Kinetic Probe Competition Assays (kPCA)

The basic principle of this assay is explained in [34]. Prior to each experiment, 6 µL of fluorescent probe (final concentration 15 nM) was dispensed to the "assay-ready" plates containing 100 nl of compound dilutions using a Multidrop Combi and the injection system of the PHERAstar FS plate reader was washed with $NaOH/H_20$ and primed with Tag-lite™ GnRH cells. Finally, the assay plates were introduced into the instrument, 4 µl of cells (1000 cells/µl) were rapidly dispensed with the syringe to each well and the TR-FRET signals corresponding to the competitive binding of probe and test compounds were recorded as described under *TR-FRET Probe Equilibrium Assays* with kinetic intervals of 78 seconds.

Data Analysis

All experimental data were analyzed using the nonlinear regression curve-fitting program GraphPad Prism v. 5.00 (GraphPad Software Inc., San Diego, CA). Further details on the handling of TR-FRET data are available in [34].

For radioligand binding assays, the previously reported K_D value of 0.35 nM for ^{125}I-triptorelin [32] was used to convert IC_{50} values obtained from competition curve analysis into K_i values with the help of the Cheng-Prusoff equation [35]:

$$K_i = IC_{50}/(1+[\text{radioligand}]/K_D)$$

Likewise, a K_D value of 0.8 nM obtained for the "red"-labeled buserelin by fitting the data from the TR-FRET Probe Equilibrium Binding Assay (Supplementary Figure S1) to the

model “One site – Specific binding”, was used to convert IC_{50} values from TR-FRET experiments to K_i values.

The observed association rates (k_{obs}) derived from both assays were obtained by fitting association data using one phase exponential association. The dissociation rates were obtained by fitting dissociation data to a one phase exponential decay model. The k_{obs} values were converted into association rate (k_{on}) values using the following equation:

$k_{on} = (k_{obs} – k_{off})/[radioligand]$

The association and dissociation rates were used to calculate the kinetic K_D using the following equation:

$K_D = k_{off}/k_{on}$

To further validate probe affinity and kinetic rate constants, association data from kinetic probe titration experiments were fitted to the ‘’Association kinetics – two or more concentrations of hot’’ model (Supplementary Figure S2). The obtained k_{on} from these experiments and K_D from equilibrium binding was used to calculate k_{off} as described above.

Association and dissociation rates for unlabeled ligands were calculated by fitting the data of the competition association assay using kinetics of competitive binding [33]:

$$K_A = k_1[L]\cdot 10^{-9} + k_2$$
$$K_B = k_3[I]\cdot 10^{-9} + k_4$$
$$S = \sqrt{(K_A - K_B)^2 + 4\cdot k_1 \cdot k_3 \cdot L \cdot I \cdot 10^{-18}}$$
$$K_F = 0.5(K_A + K_B + S)$$
$$K_S = 0.5(K_A + K_B - S)$$
$$Q = \frac{B_{\max} \cdot k_1 \cdot L \cdot 10^{-9}}{K_F - K_S}$$
$$Y = Q \cdot \left(\frac{k_4 \cdot (K_F - K_S)}{K_F \cdot K_S} + \frac{k_4 - K_F}{K_F} e^{(-K_F \cdot X)} - \frac{k_4 - K_S}{K_S} e^{(-K_S \cdot X)}\right)$$

Where k_1 is the k_{on} of the radioligand ($M^{-1}min^{-1}$), k_2 is the k_{off} of the radioligand (min^{-1}), L is the radioligand concentration (nM), I is the concentration of the unlabeled competitor (nM), X is the time (min) and Y is the specific binding of the radioligand (DPM). During a

competition association these parameters are set, obtaining k_1 from the control curve without competitor and k_2 from previously performed dissociation assays described under *Radioligand Association and Dissociation Assays*. With that the k_3, k_4 and B_{max} can be calculated, where k_3 represents the k_{on} ($M^{-1}min^{-1}$) of the unlabeled ligand, k_4 stands for the k_{off} of the unlabeled ligand and B_{max} equals the total binding (DPM). All competition association data were globally fitted.

In case of kPCA, the kinetics of the competitive binding model was enhanced with a mathematical term describing a mono-exponential decay that accounts for signal drift [34]. As stated for the radioligand binding assays, the kinetic rate constants of the fluorescent probe (k_1 and k_2) were determined in separate experiments and set constant in kPCA data analysis.

The residence time (RT) was calculated as in the following equation:

$$RT = 1/k_{off}$$

All values obtained from radioligand binding assays are means of at least three independent experiments performed in duplicate, unless stated otherwise. Values obtained from TR-FRET assays are means of two independent experiments performed in quadruplicate, unless stated otherwise.

Results

Determination of the association and dissociation rate constants of ^{125}I-triptorelin

The binding properties of ^{125}I-triptorelin to CHOhGnRH membranes were quantified with traditional kinetic radioligand binding assays. Association and dissociation experiments provided k_{on} and k_{off} values of 0.4 ± 0.1 $nM^{-1}min^{-1}$ and 0.05 ± 0.0004 min^{-1}, respectively (Figure 1A and Table 2). From these data the equilibrium dissociation constant (kinetic K_D) was calculated, which had a value of 0.2 nM.

Determination of the association and dissociation rate constants of the fluorescently labeled buserelin derivative probe

A fluorescently labeled buserelin derivative was used as a probe in all TR-FRET assays. The kinetic parameters of the fluorescent tracer were determined by performing association and dissociation experiments. Experiments yielded a k_{on} and k_{off} of 0.008 ± 0.001 $nM^{-1}min^{-1}$ and 0.01 ± 0.001 min^{-1}, respectively (Figure 1B, Table 3, Supplementary Figure 2). The kinetic K_D value calculated from these experiments was 1.2 nM.

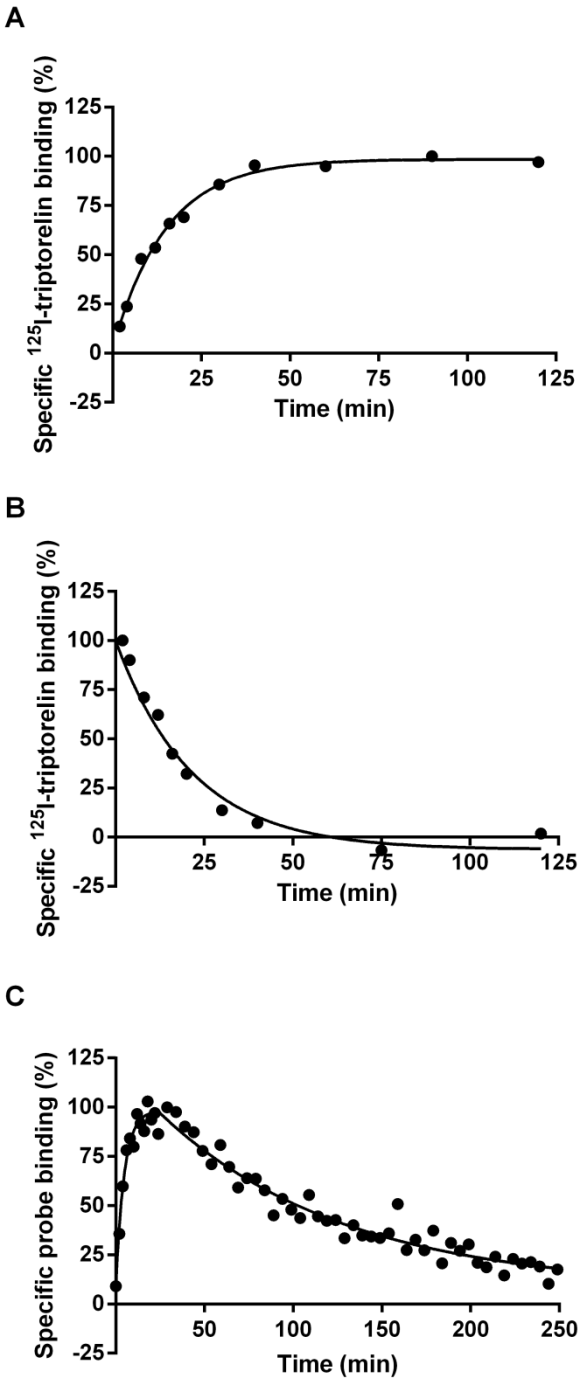

Figure 1: Association and dissociation kinetics of ^{125}I-triptorelin (A and B, respectively) or fluorescent probe (C) at the hGnRH receptor. Representative graphs from one experiment performed in duplicate (see Table 2 and 3 for kinetic parameters).

Table 2: Comparison of the affinity, dissociation constants and kinetic parameters of reference agonist triptorelin obtained with different radioligand binding assays

Assay	**pK_D[b] and (K_D (nM))**	**pK_i and (K_i (nM))**	**k_{on} (nM^{-1} min^{-1})**	**k_{off} (min^{-1})**
Displacement	N.A.	9.6 ± 0.09 (0.27)	N.A.	N.A.
Association and dissociation	9.9 ± 0.11 (0.13)	N.A.	0.40 ± 0.12	0.050 ± 0.0004
Competition association[a]	9.7 ± 0.12 (0.22)	N.A.	0.12 ± 0.014	0.026 ± 0.008

Values are means ± SEM of three separate experiments performed in duplicate. N.A., not applicable. [a]The binding kinetics of unlabeled triptorelin were determined by addition of 0.3-, 1- and 3-fold its K_i value. [b]$K_D = k_{off}/k_{on}$

Table 3: Comparison of the affinity, dissociation constants and kinetic parameters of the fluorescent buserelin probe obtained with different TR-FRET assays

Assay	**pK_D and (K_D (nM))**	**pK_i and (K_i (nM))**	**k_{on} (nM^{-1} min^{-1})**	**k_{off} (min^{-1})[b]**
Equilibrium association	9.1 ± 0.8 (0.8)	N.A.	N.A.	N.A.
Association and dissociation[a]	8.9 ± 0.9 (1.2)	N.A.	0.008 ± 0.001	0.010 ± 0.001
Multiple association and dissociation	8.7 ± 0.06 (2.1)	N.A.	0.008 ± 0.001	0.016 ± 0.002

Values are means ± SEM of three separate experiments. N.A., not applicable. [a]The dissociation kinetics of fluorescently labeled buserelin derivative were determined by addition of 10 µM buserelin. [b] $k_{off} = K_D$(equilibrium)$/k_{on}$

Determination of the binding affinity of hGnRHR agonists with ^{125}I-triptorelin

Equilibrium radioligand binding assays were performed to assess the ability of twelve GnRH analogues to displace ^{125}I-triptorelin from CHOhGnRH cell membranes. All ligands were able to fully displace ^{125}I-triptorelin in a concentration-dependent manner (Figure 2A and Table 4). All peptides had a Hill-coefficient close to unity in the ^{125}I-triptorelin displacement assay (data not shown), which indicated a competitive mode of inhibition with regard to the radioligand. Of all tested ligands nafarelin had the highest affinity for the

hGnRH receptor with a K_i value of 0.06 nM and GnRH had the lowest affinity of 13 nM. All other ligands had affinities in the low to sub-nanomolar range.

Determination of the binding affinity of hGnRHR agonists with TR-FRET

The binding affinity of twelve agonists was also determined using a fluorescently labeled buserelin derivative as a tracer and Tag-lite™ GnRH cells in a TR-FRET assay. In accordance with the radioligand binding results, all agonists were able to fully displace the fluorescent tracer from the hGnRH receptor in a concentration-dependent manner (Figure 2B and Table 4). The data were in fair agreement with the affinities determined in the radioligand displacement assay despite the inherent differences between the two assays (r^2=0.5 and p<0.05) (Figure 4C).

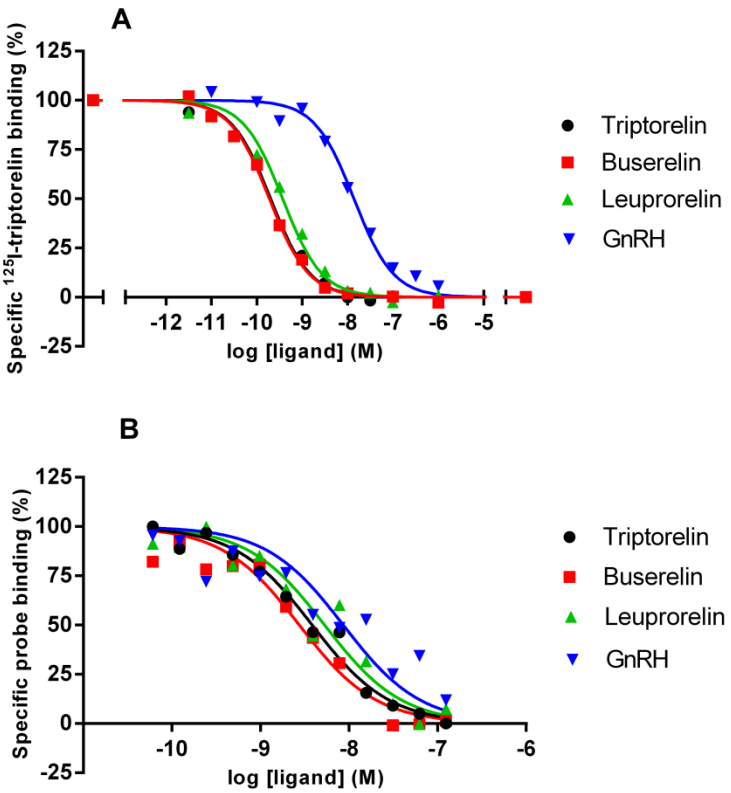

Figure 2: Displacement of ^{125}I-triptorelin (A) or fluorescent probe (B) from the hGnRH receptor by the twelve peptide agonists. Representative graphs from one experiment performed in duplicate (see Table 4 for affinity values)**.**

Validation and optimization of the competition association assay with ^{125}I-triptorelin

With the k_{on} and k_{off} values of ^{125}I-triptorelin obtained from traditional association and dissociation experiments, the k_{on} (k_3) and k_{off} (k_4) values of unlabeled triptorelin could be determined by fitting the kinetic parameters into the model of 'kinetics of competitive binding' as described under *'Material & Methods'*. Three different concentrations of unlabeled triptorelin were tested and presented a shared k_{on} (k_3) and k_{off} (k_4) value of 0.1 ± 0.01 $nM^{-1}min^{-1}$ and 0.03 ± 0.008 min^{-1}, respectively (Figure 3A). These values were in good agreement with the association and dissociation rates obtained with traditional kinetic experiments (Table 2). Additionally, a comparison of the affinity (0.3 nM) and dissociation

constants (0.1 nM and 0.2 nM), acquired from equilibrium and kinetic experiments respectively, further confirmed the competition association assay as a valid tool to determine the binding kinetics of unlabeled ligands at the hGnRH receptor (Table 2).

To improve the throughput of this assay, one concentration of competitor was selected that yielded an assay window discernable from both the baseline and control curve (i.e. specific binding approximately 40-60%). In this case, a concentration of competitor equal to 1-fold its K_i value presented the best assay window. Analysis of this single concentration showed similar kinetic rates for triptorelin in comparison to the three-concentration method, which were statistically indifferent (data not shown; $p>0.05$). Thus, this one-concentration method was used for subsequent determination of the binding kinetics of other unlabeled hGnRHR peptide agonists.

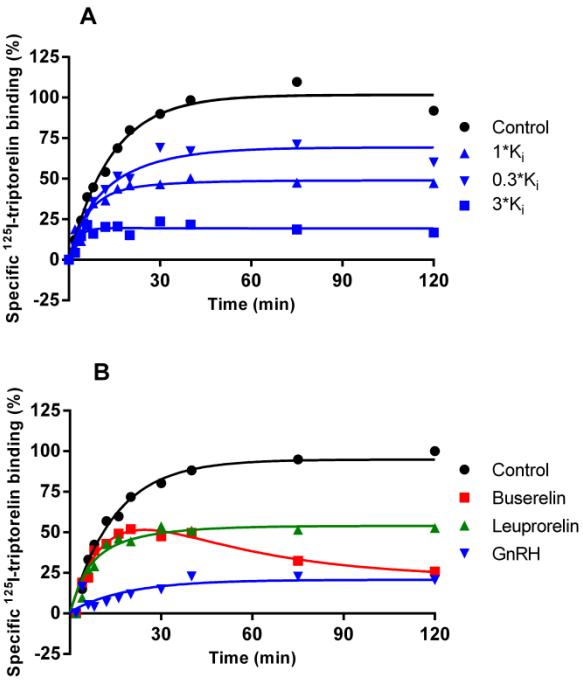

Figure 3: Competition association experiment with ^{125}I-triptorelin in the absence or presence of 0.3, 1 or 3*K_i value of unlabeled triptorelin (A) or 1*K_i value of buserelin, leuprorelin or GnRH (B). Representative graphs from one experiment performed in duplicate (See Table 2 for kinetic parameters).

Determination of the receptor binding kinetics of unlabeled hGnRHR agonists with ^{125}I-triptorelin

By use of the one-concentration competition association assay the binding kinetics of 11 other unlabeled hGnRHR agonists were quantified (Figure 3B, Table 5). Juxtaposing affinities (K_i values) and dissociation constants (K_D values) acquired from equilibrium and kinetic experiments resulted in a high correlation ($r^2 = 0.9$, $p<0.0001$). Firstly, this further confirmed that the competition association assay was a valid tool to determine the binding kinetics of unlabeled ligands for the hGnRH receptor (Figure 4A) and secondly, proved that equilibrium was reached for all agonists in the displacement experiments. The dissociation rates ranged from 0.2 ± 0.03 min^{-1} for goserelin to 0.01 ± 0.003 min^{-1} for buserelin, a variance of roughly 20-fold. Interestingly, three distinctive association patterns were obtained from the

competition association assays (Figure 3B). Firstly, an 'overshoot' in ^{125}I-triptorelin association was observed for slowly dissociating compounds, such as buserelin. Secondly, we noticed a shallow increase in ^{125}I-triptorelin association for rapidly dissociating compounds, such as GnRH, and lastly, no difference was observed in the shape of the ^{125}I-triptorelin association curve for equally fast-dissociating compounds, such as leuprorelin. The observed differences in dissociation kinetics were all in comparison to those of the radioligand ^{125}I-triptorelin (Figure 3B). Association rates ranged from 0.8 ± 0.2 $nM^{-1}min^{-1}$ for nafarelin to 0.02 ± 0.004 $nM^{-1}min^{-1}$ for fertirelin, a span of approximately 35-fold.

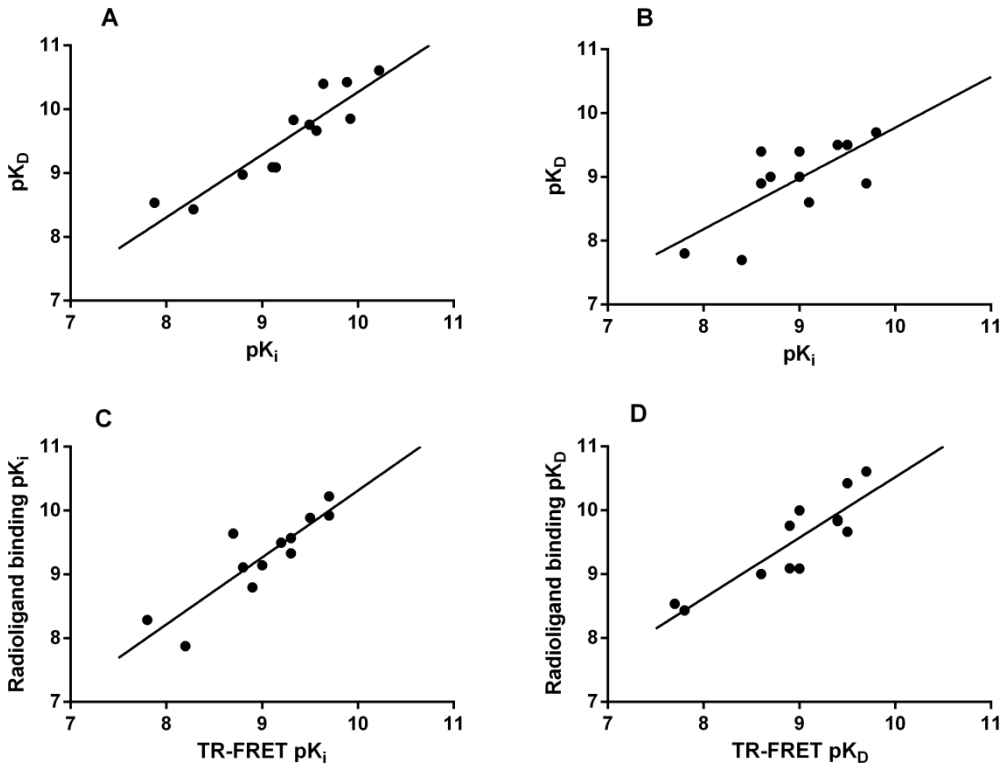

Figure 4: Correlation between affinities (pK_i) and dissociation constants (pK_D) derived from (A) radioligand binding (r^2= 0.9, P<0.0001) and (B) TR-FRET experiments (r^2=0.5, P<0.05). (C) Correlation between affinities (pK_i) derived from radioligand binding and HTRF experiments (r^2=0.5, P<0.05). (D) Correlation between dissociation constants (pK_D) derived from radioligand binding and TR-FRET experiments (r^2=0.8, P<0.001). In all cases, pK_i values were obtained from equilibrium displacement studies and pK_D values were determined with competition association experiments.

Determination of the receptor binding kinetics of unlabeled hGnRHR agonists with a fluorescently labeled buserelin derivative

Table 4: Binding parameters of GnRH peptide agonists derived from radioligand binding and TR-FRET experiments

	Radioligand binding		**TR-FRET**	
Agonist	**pK_i and (K_i (nM))**	**pK_D and (K_D (nM))**	**pK_i and (K_i (nM))**	**pK_D and (K_D (nM))**
GnRH	7.9 ± 0.05 (13)	8.5 ± 0.08 (2.9)	8.4 ± 0.6 (4.0)	7.7 ± 0.03 (22)
Triptorelin	9.6 ± 0.09 (0.3)	9.7 ± 0.1 (0.2)	9.5 ± 0.2 (0.4)	9.5 ± 0.03 (0.4)
[D-Ala^6]-GnRH	9.0 ± 0.05 (0.8)	9.1 ± 0.09 (0.8)	8.6 ± 0.4 (2.3)	8.9 ± 0.02 (1.3)
[D-Lys^6]-GnRH	8.3 ± 0.1 (5.2)	8.4 ± 0.2 (3.7)$^{\#}$	7.8 ± 0.3 (16)	7.8 ± 0.01 (15)
Fertirelin	9.2 ± 0.05 (0.7)	9.1 ± 0.08 (0.8)$^{\#}$	9.0 ± 0.3 (1.0)	9.0 ± 0.02 (0.9)
Alarelin	9.4 ± 0.1 (0.5)	9.8 ± 0.1 (0.2)	9.0 ± 0.3 (0.9)	9.4 ± 0.03 (0.4)
Deslorelin	10 ± 0.1 (0.1)	9.9 ± 0.1 (0.1) $^{\#}$	8.6 ± 0.6 (0.8)	9.4 ± 0.04 (0.4)
Leuprorelin	9.5 ± 0.09 (0.3)	9.8 ± 0.1 (0.2)	9.7 ± 0.3 (0.2)	8.9 ± 0.03 (1.2)
Nafarelin	10 ± 0.06 (0.06)	10.6 ± 0.1 (0.03)	9.8 ± 0.3 (0.2)	9.7 ± 0.06 (0.2)
Buserelin	9.9 ± 0.05 (0.1)	10.4 ± 0.2 (0.04)	9.4 ± 0.2 (0.4)	9.5 ± 0.04 (0.3)
Goserelin	8.8 ± 0.06 (1.6)	9.0 ± 0.08 (1.1)	9.1 ± 0.3 (0.9)	8.6 ± 0.02 (2.7)
Histerelin	9.8 ± 0.2 (0.2)	10 ± 0.08 (0.04)	8.7 ± 0.5 (1.9)	9.0 ± 0.04 (1.0)

Values are means ± SEM of at least three separate experiments performed in duplicate. $^{\#}$Values are means ± SEM of two separate experiments performed in duplicate. $K_D = k_{off}/k_{on}$

The kinetic parameters of the twelve GnRH agonists were also determined with TR-FRET experiments (Figure 5, Table 5 and Supplementary Figure 3). Association rates ranged from 0.1 ± 0.02 $nM^{-1}min^{-1}$ for triptorelin to 0.02 ± 0.002 $nM^{-1}min^{-1}$ for histerelin. Buserelin was again one of the slowest dissociating agonists with a dissociation rate of 0.02 ± 0.003 min^{-1}, while GnRH had the fastest dissociation rate of 0.4 ± 0.03 min^{-1}. The dissociation constants (K_D) calculated from k_{on} and k_{off} values were consistent with the affinities determined in HTRF displacement assays (Figure 4B) as well as with the K_D values obtained from the radioligand binding studies (Figure 4D). Dissociation rate constants (k_{off}) were in good agreement with the data obtained from radioligand binding experiments (r^2=0.7, p<0.0005) (Figure 6A), while the association rates (k_{on}) presented no correlation (r^2=0.03, p=0.6) (Figure 6B).

Discussion and Conclusions

Over the years several studies have indicated that long duration of action is an important feature contributing to improved efficacy of drugs designed to treat chronic illness. Moreover, increased target-residence time offers the potential for a once-daily dosage form

that increases patient compliance which is crucial for the management of diseases [1, 2, 5, 36-40].

The GnRH receptor is the target of multiple marketed peptide agonists, classified as functional antagonists, used to treat hormone-dependent diseases. Available patient information for the most commonly prescribed GnRH analogues suggests that the PK/PD profiles are very similar. Hence, knowledge of the *in vitro* binding kinetics could give extra insights into these well-known drugs. However, the potential impact of variable binding kinetics of these GnRH peptide derivatives on clinical efficacy has not been investigated. Aside from agonists, a few studies have detailed the effect of slow dissociation kinetics of

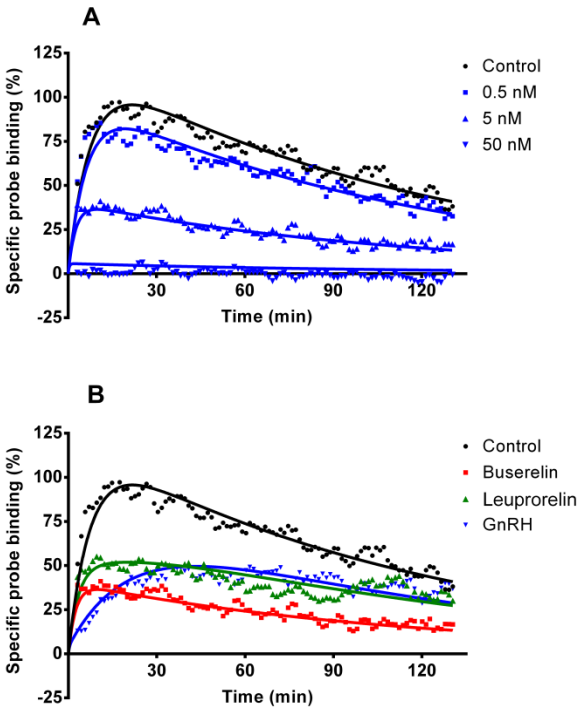

Figure 5: Competition association experiment with fluorescent probe in the absence or presence of increasing concentrations of buserelin (A) or one-concentration of unlabeled agonist that showed around 50% displacement (B). Representative graphs from one experiment performed in quadruplicate.

antagonists for the GnRH receptor to decrease the maximal response of an agonist (insurmountability) *in vitro* and to improve and prolong efficacy *in vivo*. A study of Kohout and coworkers [25] addressed the insurmountability of a small molecule GnRH antagonist, TAK-013. The authors examined the differences in antagonistic and kinetic properties of TAK-013 for hGnRHR, mouse GnRHR (mGnRHR) and mutated mGnRHR and found a good correlation between the degree of insurmountability in *in vitro* functional assays and the dissociation rate from the receptor. Therefore, they proposed slow receptor dissociation kinetics to be accountable for the mechanism of insurmountability of TAK-013. Similar findings were published [24] for another series of small molecule antagonists, i.e. uracils. Slowly dissociating ligands displayed insurmountable antagonism whereas faster dissociating ligands proved to be surmountable antagonists. To determine the dissociation rates of these uracil-series of antagonists the competition association method [33] was used with a proprietary small molecule radioligand as a tracer. Such a competition association assay has recently been applied to determine the receptor kinetics of ligands for several different GPCRs such as the adenosine A_{2A} receptor [41], the muscarinic M_3 receptor [42], the chemokine receptor CCR2 [43] and the

histamine H_1 and H_3 receptor [44]. We were able, for the first time, to determine the kinetic parameters of twelve GnRH peptide agonists, including many marketed drugs.

Two different techniques were applied, namely; radioligand binding studies and kinetic probe competition assays (kPCA) with a TR-FRET read-out. For the former, a comparison of the radioligand's kinetic parameters obtained from traditional radioligand binding experiments showed a good consistency with the kinetic parameters for triptorelin derived from the competition association assay (Table 2). Moreover, the kinetics of the 11 remaining GnRH agonists presented a good correlation between the kinetically derived K_D and the affinity obtained from equilibrium radioligand binding studies (Figure 4). Secondly, we also conducted these experiments with a fluorescently labeled buserelin probe in a TR-FRET assay. This technology has already been used for examining equilibrium GPCR ligand binding [45, 46] and more recently it was used to characterize the binding kinetics of the Histamine H1 receptor [34].

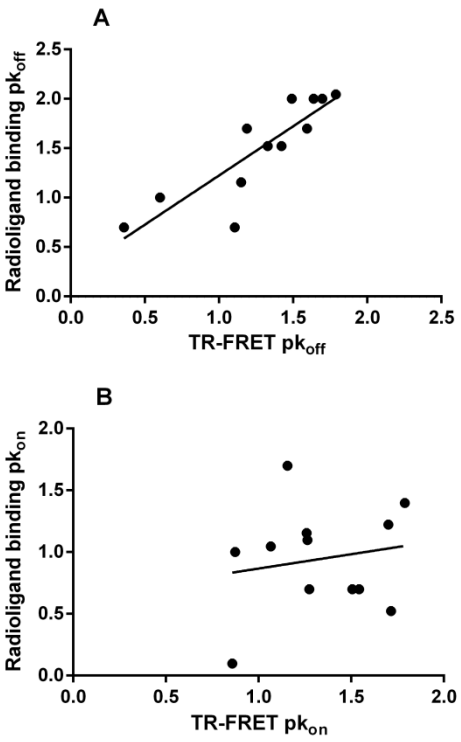

Figure 6: Correlation between the kinetic parameters obtained from radioligand binding assays and kPCA TR-FRET experiments. (A) Dissociation rate (k_{off}) (r^2=0.7, P<0.0005); (B) association rate (k_{on}) (r^2=0.03, P=0.6).

Comparing affinities and kinetic K_D values from both the radioligand binding and TR-FRET assays yielded significant correlations demonstrating a good reproducibility between both techniques. The two distinct assays also proved to be very amenable to the determination of the kinetic receptor binding parameters of (peptide) GnRH agonists. Dissociation rates, and thus residence times, between assays were in good accordance with p values of <0.0005, while the association rates were in less agreement between techniques. It should be noted that the experimental differences between both assays are considerable, which may have consequences for the kinetic parameters derived in the two assays. For example, the radioligand binding studies were manually dispensed while the TR-FRET assays were performed using automated dispensing devices. It has been reported that compound handling can be an important source of assay variability [47]. In addition, the kinetic binding parameters were determined using a one-concentration method for the

radioligand binding experiments whereas the kPCA studies used five different concentrations.

Table 5: Kinetic receptor binding parameters of GnRH peptide agonists derived from radioligand binding competition association assays and kPCA TR-FRET experiments

	Radioligand binding			**TR-FRET**		
Agonist	**k_{on} ($nM^{-1}min^{-1}$)[a]**	**k_{off} (min^{-1})[a]**	**RT (min)[c]**	**k_{on} ($nM^{-1}min^{-1}$)[b]**	**k_{off} (min^{-1})[b]**	**RT (min)[c]**
GnRH	0.06 ± 0.01	0.2 ± 0.02	6.3 ± 0.6	0.02 ± 0.01	0.44 ± 0.3	2.3 ± 1.6
Triptorelin	0.1 ± 0.01	0.03 ± 0.008	39 ± 12	0.1 ± 0.02	0.05 ± 0.008	21 ± 3.7
[D-Ala^6]-GnRH	0.08 ± 0.01	0.07 ± 0.01	15 ± 3.1	0.05 ± 0.007	0.07 ± 0.01	14 ± 2.3
[D-Lys^6]-GnRH	0.04 ± 0.02[#]	0.1 ± 0.04[#]	7.7 ± 2.3[#]	0.02 ± 0.01	0.25 ± 0.17	4 ± 2.6
Fertirelin	0.02 ± 0.004[#]	0.02 ± 0.001[#]	56 ± 3.1[#]	0.07 ± 0.009	0.06 ± 0.01	15 ± 2.4
Alarelin	0.09 ± 0.02	0.01 ± 0.002	77 ± 12	0.09 ± 0.009	0.03 ± 0.005	31 ± 4.8
Deslorelin	0.07 ± 0.01[#]	0.01 ± 0.002[#]	100 ± 20[#]	0.05 ± 0.005	0.02 ±0.004	44 ± 6.9
Leuprorelin	0.2 ± 0.04	0.03± 0.005	36 ± 6.4	0.03 ± 0.004	0.04 ± 0.006	26 ± 4.4
Nafarelin	0.8 ± 0.2	0.02 ± 0.003	50 ± 7.5	0.1 ± 0.02	0.03 ± 0.006	39 ± 9.8
Buserelin	0.2 ± 0.06	0.009 ± 0.003	111 ± 37	0.05 ± 0.004	0.02 ± 0.003	61 ± 10
Goserelin	0.2 ± 0.002	0.2 ± 0.03	5.6 ± 0.8	0.03 ± 0.005	0.08 ± 0.01	13 ± 2.4
Histerelin	0.3 ± 0.04	0.01 ± 0.002	83 ± 14	0.02 ± 0.002	0.02 ± 0.004	50 ± 8.8

Values are means ± SEM of at least three separate experiments performed in duplicate. [#]Values are means ± SEM of two separate experiments performed in duplicate. [a]k_{on} and k_{off} of unlabeled GnRH agonists were determined at 1-fold K_i concentrations. [b]k_{on} and k_{off} of unlabeled GnRH agonists were determined at 0.5, 5, 50 and 500 nM. [c]$RT = 1/k_{off}$

Another notable difference is that in the radioligand binding studies CHOhGnRH membranes were used whereas the TR-FRET assays were performed with Tag-lite™ HEK_{293} GnRH cells. Packeu *et al.* discussed the differences in membrane interactions of membrane preparations and whole cells and their effects on binding kinetics for the D_{2L}-dopamine receptors [48]. Moreover, the authors found slower dissociation rates from intact cells in comparison to membrane preparations and they proposed that an intact cellular environment could play a role in stabilizing the D_{2L}-dopamine receptors in a particular conformation. A similar reasoning might be applicable to the GnRH receptor, although in our case the receptor appears in a way that slows down the association rates of the peptides (Table 5). It

may also be that the peptides simply have more difficulty in reaching the receptor on intact cells than on membrane fragments.

It might be argued that the assay temperature of 25 °C is not representative for binding kinetics observed in vivo. For example, Sakai [49] examined the effect of temperature on the dissociation of ^{125}I-prolactin from the rabbit mammary gland prolactin receptor. They found a linear relationship between the dissociation rate and temperature with an increased dissociation rate at higher temperatures. Another study [50] also showed that the dissociation of [^{3}H]-QMDP from the histamine H_1 receptor was temperature-dependent, which was also true for the association rate but to a lesser extent. Arrhenius plots for both the association rate and dissociation rate of [^{3}H]-QMDP were linear between 6 °C and 37 °C. It should be noted that, although these studies show a linear increase in dissociation rates with higher temperatures the slope of this increase could be very different between targets and their ligands. Taken together, this indicates that the kinetic ranking of ligands for the same receptor can be expected to stay the same over different temperatures. Therefore, even though all our experiments were performed at 25 °C, the results are still of great value for translation to *in vivo* outcomes.

Numerous peptide GnRH derivatives have been synthesized and studied for their so-called structure-affinity relationships (SAR), with the aim to improve their affinity, potency and/or metabolic stability [20-22, 51-53] In summary, it was established that the NH_2-terminal domain (pGlu-His-Trp-Ser) of GnRH is important for receptor binding and activation with Trp^3 as a critical residue. In addition, the COOH-terminal domain (Pro-Gly-NH_2) is crucial for receptor binding where substitution of Pro^9 or removal of NH_2 results in very low affinity unless the COOH-terminal tail is substituted for an ethylamide which also improves metabolic stability. In contrast, the central domain of the peptide is less conserved and studies show that exchange of Tyr^5, Leu^7 or Arg^8 is mostly well tolerated. The most beneficial substitution is that of Gly^6 with a D-amino acid which provides a more favorable conformation and in turn results in increased potency. D-amino acids at the 6th position of the peptide are therefore incorporated in all marketed GnRH analogues. The amino acid sequences of the twelve GnRH peptides tested in this study are identical with the exception of the 6th amino acid and the carboxylic tail (Table 1). A tentative structure kinetic relationship (SKR) could be established for the carboxylic tail (i.e. substitution of the glycine-amide for an ethylamide). For instance, a comparison of triptorelin and deslorelin showed 2/3-fold changes in affinity (Table 4), which was also observed in residence time. This ethylamide-induced improvement in residence time was also true to a bigger extent for goserelin and buserelin, where the affinity was improved 2- or 16-fold (TR-FRET and radioligand binding, respectively), while the residence time was more significantly affected, witnessed by a 5-fold increase in the kPCA TR-FRET experiments and a 20-fold increase in the radioligand binding studies. This shows

that shortening the carboxylic tail of the peptide slightly increases the affinity, but results in a more significant improvement in residence time. Interestingly, three decades ago it was already speculated that buserelin has a longer residence time. In these studies, the authors proposed that the high potency and long duration of action of buserelin *in vivo* was a result of prolonged GnRH receptor binding [54-56]. Along similar lines, Flanagan and coworkers discussed slower dissociation rates of GnRH agonists with a more hydrophobic amino acid at position 6 [57]. However, no mechanism or kinetic binding data was reported at that time.

Previously published mutagenesis studies further strengthen our hypothesis indicating the importance of the ethylamide at the carboxylic tail. Davidson and coworkers showed that the $Asn^{2.65(102)}$ residue located near the extracellular end of TM2 plays a role in ligand binding, specifically with the carboxylic tail of GnRH analogs [58]. Mutations to alanine at this position significantly decreased the potency of GnRH analogs with Gly^{10}-NH_2, but had a lesser effect on GnRH analogs with an ethylamide tail [21, 59, 60]. It may be hypothesized that substitution of Gly^{10}-NH_2 with an ethylamide moiety creates less steric hindrance and increases hydrophobicity, thereby improving the fit of the agonist and thus elongating its residence time on the receptor.

In conclusion, two novel competition association assays were successfully developed and applied to determine the kinetic binding characteristics of twelve peptide agonists, including many marketed drugs targeting the GnRH receptor. All agonists proved to have high affinity for the GnRH receptor whereas significant differences were observed in their binding kinetics. These findings provide new insights and tools for the development of improved drugs targeting the GnRH receptor by incorporating optimized kinetic binding parameters. They also suggest that bringing this knowledge on kinetics to the clinic may help in improving or adjusting treatment protocols with better patient outcomes.

References

1. Zhang, R. and F. Monsma, *The importance of drug-target residence time.* Current opinion in drug discovery & development, 2009. **12**(4): p. 488-96.
2. Copeland, R.A., D.L. Pompliano, and T.D. Meek, *Drug-target residence time and its implications for lead optimization.* Nature reviews. Drug discovery, 2006. **5**(9): p. 730-9.
3. Swinney, D.C., *Biochemical mechanisms of drug action: what does it take for success?* Nature reviews. Drug discovery, 2004. **3**(9): p. 801-8.
4. Tummino, P.J. and R.A. Copeland, *Residence time of receptor-ligand complexes and its effect on biological function.* Biochemistry, 2008. **47**(20): p. 5481-92.
5. Guo, D., et al., *Drug-target residence time-a case for G protein-coupled receptors.* Medicinal research reviews, 2014. **34**(4): p. 856-92.
6. Anthes, J.C., et al., *Biochemical characterization of desloratadine, a potent antagonist of the human histamine H(1) receptor.* European journal of pharmacology, 2002. **449**(3): p. 229-37.
7. Maillard, M.P., et al., *In vitro and in vivo characterization of the activity of telmisartan: an insurmountable angiotensin II receptor antagonist.* The Journal of pharmacology and experimental therapeutics, 2002. **302**(3): p. 1089-95.
8. Kakar, S.S., W.E. Grizzle, and J.D. Neill, *The Nucleotide-Sequences of Human Gnrh Receptors in Breast and Ovarian-Tumors Are Identical with That Found in Pituitary.* Molecular and cellular endocrinology, 1994. **106**(1-2): p. 145-149.
9. von Alten, J., et al., *GnRH analogs reduce invasiveness of human breast cancer cells.* Breast Cancer Research and Treatment, 2006. **100**(1): p. 13-21.
10. Aguilar-Rojas, A., et al., *Gonadotropin-releasing hormone receptor activates GTPase RhoA and inhibits cell invasion in the breast cancer cell line MDA-MB-231.* BMC cancer, 2012. **12**: p. 550-561.
11. Angelucci, C., et al., *GnRH receptor expression in human prostate cancer cells is affected by hormones and growth factors.* Endocrine, 2009. **36**(1): p. 87-97.
12. Stojilkovic, S.S., J. Reinhart, and K.J. Catt, *Gonadotropin-releasing hormone receptors: structure and signal transduction pathways.* Endocrine reviews, 1994. **15**(4): p. 462-99.
13. Belchetz, P.E., et al., *Hypophysial responses to continuous and intermittent delivery of hypopthalamic gonadotropin-releasing hormone.* Science, 1978. **202**(4368): p. 631-3.
14. Lahlou, N., et al., *Gonadotropin and alpha-subunit secretion during long term pituitary suppression by D-Trp6-luteinizing hormone-releasing hormone microcapsules as treatment of precocious puberty.* The Journal of clinical endocrinology and metabolism, 1987. **65**(5): p. 946-53.
15. Labrie, F., *GnRH agonists and the rapidly increasing use of combined androgen blockade in prostate cancer.* Endocrine-related cancer, 2014: p. 301-317.
16. Leone Roberti Maggiore, U., et al., *Triptorelin for the treatment of endometriosis.* Expert Opin Pharmacother, 2014. **15**(8): p. 1153-79.
17. Depalo, R., et al., *GnRH agonist versus GnRH antagonist in in vitro fertilization and embryo transfer (IVF/ET).* Reprod Biol Endocrinol, 2012. **10**: p. 26.

18. Heitman, L.H. and A.P. IJzerman, *G protein-coupled receptors of the hypothalamic-pituitary-gonadal axis: a case for Gnrh, LH, FSH, and GPR54 receptor ligands.* Medicinal research reviews, 2008. **28**(6): p. 975-1011.
19. Millar, R.P. and C.L. Newton, *Current and future applications of GnRH, kisspeptin and neurokinin B analogues.* Nat Rev Endocrinol, 2013. **9**(8): p. 451-66.
20. Sealfon, S.C., H. Weinstein, and R.P. Millar, *Molecular mechanisms of ligand interaction with the gonadotropin-releasing hormone receptor.* Endocrine reviews, 1997. **18**(2): p. 180-205.
21. Millar, R.P., et al., *Gonadotropin-releasing hormone receptors.* Endocr rev, 2004. **25**(2): p. 235-275.
22. Karten, M.J. and J.E. Rivier, *Gonadotropin-Releasing-Hormone Analog Design - Structure-Function Studies toward the Development of Agonists and Antagonists - Rationale and Perspective.* Endocrine reviews, 1986. **7**(1): p. 44-66.
23. Heise, C.E., S.K. Sullivan, and P.D. Crowe, *Scintillation proximity assay as a high-throughput method to identify slowly dissociating nonpeptide ligand binding to the GnRH receptor.* Journal of biomolecular screening, 2007. **12**(2): p. 235-9.
24. Sullivan, S.K., et al., *Kinetics of nonpeptide antagonist binding to the human gonadotropin-releasing hormone receptor: Implications for structure-activity relationships and insurmountable antagonism.* Biochemical pharmacology, 2006. **72**(7): p. 838-49.
25. Kohout, T.A., et al., *Trapping of a nonpeptide ligand by the extracellular domains of the gonadotropin-releasing hormone receptor results in insurmountable antagonism.* Molecular pharmacology, 2007. **72**(2): p. 238-47.
26. Romero, E., et al., *Pharmacokinetic/pharmacodynamic model of the testosterone effects of triptorelin administered in sustained release formulations in patients with prostate cancer.* The Journal of pharmacology and experimental therapeutics, 2012. **342**(3): p. 788-98.
27. Lewis, K.A., et al., *A single histrelin implant is effective for 2 years for treatment of central precocious puberty.* The Journal of pediatrics, 2013. **163**(4): p. 1214-6.
28. Goericke-Pesch, S., et al., *Treatment of queens in estrus and after estrus with a GnRH-agonist implant containing 4.7 mg deslorelin; hormonal response, duration of efficacy, and reversibility.* Theriogenology, 2013. **79**(4): p. 640-6.
29. Aydiner, A., et al., *Two different formulations with equivalent effect? Comparison of serum estradiol suppression with monthly goserelin and trimonthly leuprolide in breast cancer patients.* Medical oncology, 2013. **30**(1): p. 354-362.
30. Alexander, S.P.H., et al., *The Concise Guide to Pharmacology 2013/14: G Protein-Coupled Receptors.* British Journal of Pharmacology, 2013. **170**(8): p. 1459-1581.
31. Smith, P.K., et al., *Measurement of protein using bicinchoninic acid.* Analytical biochemistry, 1985. **150**(1): p. 76-85.
32. Heitman, L.H., et al., *Amiloride derivatives and a nonpeptidic antagonist bind at two distinct allosteric sites in the human gonadotropin-releasing hormone receptor.* Molecular pharmacology, 2008. **73**(6): p. 1808-15.

33. Motulsky, H.J. and L.C. Mahan, *The kinetics of competitive radioligand binding predicted by the law of mass action.* Molecular pharmacology, 1984. **25**(1): p. 1-9.
34. Schiele, F., P. Ayaz, and A. Fernandez-Montalvan, *A universal, homogenous assay for high throughput determination of binding kinetics.* Analytical biochemistry, 2014. **486C**: p. 42-49.
35. Cheng, Y. and W.H. Prusoff, *Relationship between Inhibition Constant (K1) and Concentration of Inhibitor Which Causes 50 Per Cent Inhibition (I50) of an Enzymatic-Reaction.* Biochemical pharmacology, 1973. **22**(23): p. 3099-3108.
36. Smith, D.A., B.C. Jones, and D.K. Walker, *Design of drugs involving the concepts and theories of drug metabolism and pharmacokinetics.* Medicinal research reviews, 1996. **16**(3): p. 243-66.
37. Tashkin, D.P., *Is a long-acting inhaled bronchodilator the first agent to use in stable chronic obstructive pulmonary disease?* Current opinion in pulmonary medicine, 2005. **11**(2): p. 121-8.
38. Dowling, M.R. and S.J. Charlton, *Quantifying the association and dissociation rates of unlabelled antagonists at the muscarinic M3 receptor.* British journal of pharmacology, 2006. **148**(7): p. 927-37.
39. Swinney, D.C., *The role of binding kinetics in therapeutically useful drug action.* Current opinion in drug discovery & development, 2009. **12**(1): p. 31-9.
40. Vauquelin, G. and I. Van Liefde, *Slow antagonist dissociation and long-lasting in vivo receptor protection.* Trends in pharmacological sciences, 2006. **27**(7): p. 356-9.
41. Guo, D., et al., *Functional efficacy of adenosine A_{2A} receptor agonists is positively correlated to their receptor residence time.* Br J Pharmacol, 2012. **166**(6): p. 1846-1859.
42. Sykes, D.A., M.R. Dowling, and S.J. Charlton, *Exploring the mechanism of agonist efficacy: a relationship between efficacy and agonist dissociation rate at the muscarinic M3 receptor.* Molecular pharmacology, 2009. **76**(3): p. 543-51.
43. Zweemer, A.J., et al., *Multiple binding sites for small-molecule antagonists at the CC chemokine receptor 2.* Molecular pharmacology, 2013. **84**(4): p. 551-61.
44. Slack, R.J., et al., *Pharmacological characterization of GSK1004723, a novel, long-acting antagonist at histamine H(1) and H(3) receptors.* British journal of pharmacology, 2011. **164**(6): p. 1627-41.
45. Zhang, R. and X. Xie, *Tools for GPCR drug discovery.* Acta pharmacologica Sinica, 2012. **33**(3): p. 372-84.
46. Degorce, F., et al., *HTRF: A technology tailored for drug discovery - a review of theoretical aspects and recent applications.* Current chemical genomics, 2009. **3**: p. 22-32.
47. Gubler, H., U. Schopfer, and E. Jacoby, *Theoretical and experimental relationships between percent inhibition and IC50 data observed in high-throughput screening.* J Biomol Screen, 2013. **18**(1): p. 1-13.
48. Packeu, A., et al., *Antagonist-radioligand binding to D2L-receptors in intact cells.* Biochemical pharmacology, 2008. **75**(11): p. 2192-203.
49. Sakai, S., *Effect of hormones on dissociation of prolactin from the rabbit mammary gland prolactin receptor.* Biochem J, 1991. **279 (Pt 2)**: p. 461-5.

50. Treherne, J.M. and J.M. Young, *Temperature-dependence of the kinetics of the binding of [3H]-(+)-N-methyl-4-methyldiphenhydramine to the histamine H1-receptor: comparison with the kinetics of [3H]-mepyramine.* Br J Pharmacol, 1988. **94**(3): p. 811-22.
51. Fujino, M., et al., *Syntheses and Biological-Activities of Analogs of Luteinizing-Hormone Releasing Hormone (Lh-Rh).* Biochemical and biophysical research communications, 1972. **49**(3): p. 698-705.
52. Monahan, M.W., et al., *Synthetic Analogs of Hypothalamic Luteinizing-Hormone Releasing Factor with Increased Agonist or Antagonist Properties.* Biochemistry, 1973. **12**(23): p. 4616-4620.
53. Hovelmann, S., et al., *Impact of aromatic residues within transmembrane helix 6 of the human gonadotropin-releasing hormone receptor upon agonist and antagonist binding.* Biochemistry, 2002. **41**(4): p. 1129-1136.
54. Yeo, T., et al., *Response of luteinizing hormone from columns of dispersed rat pituitary cells to a highly potent analogue of luteinizing hormone releasing hormone.* The Journal of endocrinology, 1981. **91**(1): p. 33-41.
55. Koiter, T.R., et al., *A comparison of the LH-releasing activities of LH-RH and its agonistic analogue buserelin in the ovariectomized rat.* Life sciences, 1984. **34**(16): p. 1597-604.
56. Koiter, T.R., et al., *The prolonged action of the LHRH agonist buserelin (HOE 766) may be due to prolonged binding to the LHRH receptor.* Life sciences, 1986. **39**(5): p. 443-52.
57. Flanagan, C.A., et al., *A high affinity gonadotropin-releasing hormone (GnRH) tracer, radioiodinated at position 6, facilitates analysis of mutant GnRH receptors.* Endocrinology, 1998. **139**(10): p. 4115-9.
58. Davidson, J.S., et al., *Identification of N-glycosylation sites in the gonadotropin-releasing hormone receptor: role in receptor expression but not ligand binding.* Molecular and cellular endocrinology, 1995. **107**(2): p. 241-5.
59. Hoffmann, S.H., et al., *Residues within transmembrane helices 2 and 5 of the human gonadotropin-releasing hormone receptor contribute to agonist and antagonist binding.* Molecular endocrinology, 2000. **14**(7): p. 1099-1115.
60. Davidson, J.S., et al., *Asn102 of the gonadotropin-releasing hormone receptor is a critical determinant of potency for agonists containing C-terminal glycinamide.* J Biol Chem, 1996. **271**(26): p. 15510-4.

Supplemental Data

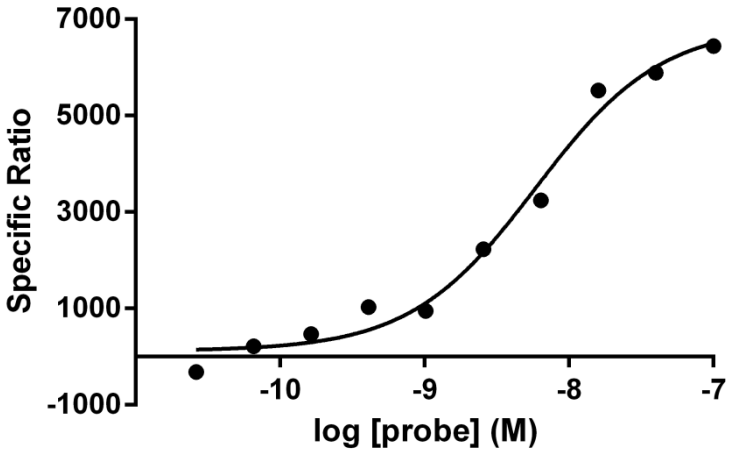

Supplementary Figure 1. Saturation equilibrium binding of fluorescent buserelin probe to Tag-lite™ GnRH cells (IC_{50} = 5.9 nM, r^2 = 0.99). Representative graph from one experiment performed in duplicate.

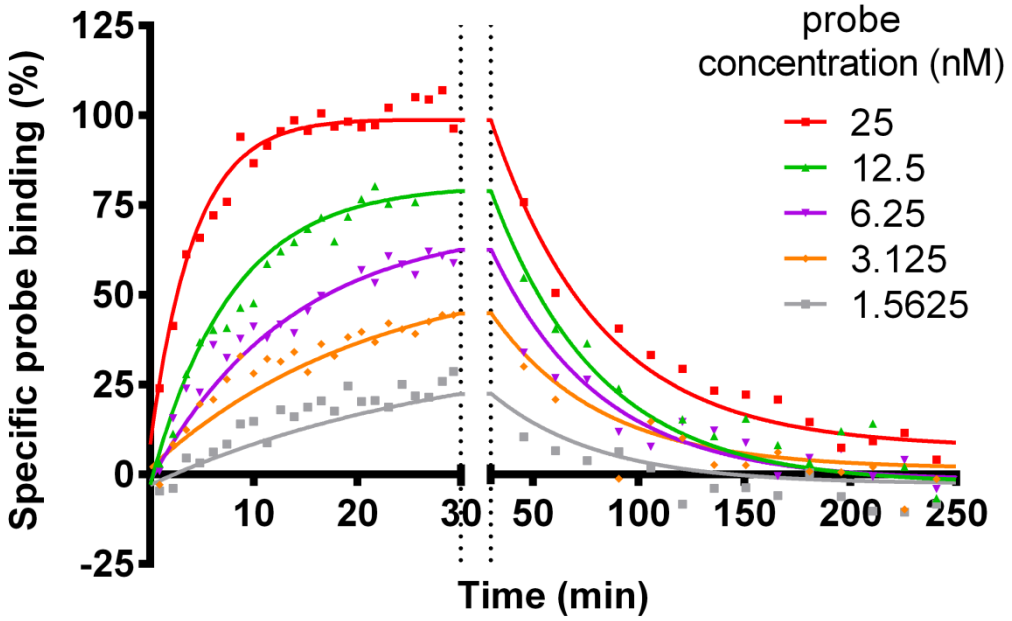

Supplementary Figure 2. Association and dissociation kinetics of five concentrations of fluorescent buserelin probe to Tag-lite™ GnRH cells. Representative graph from one experiment performed in duplicate.

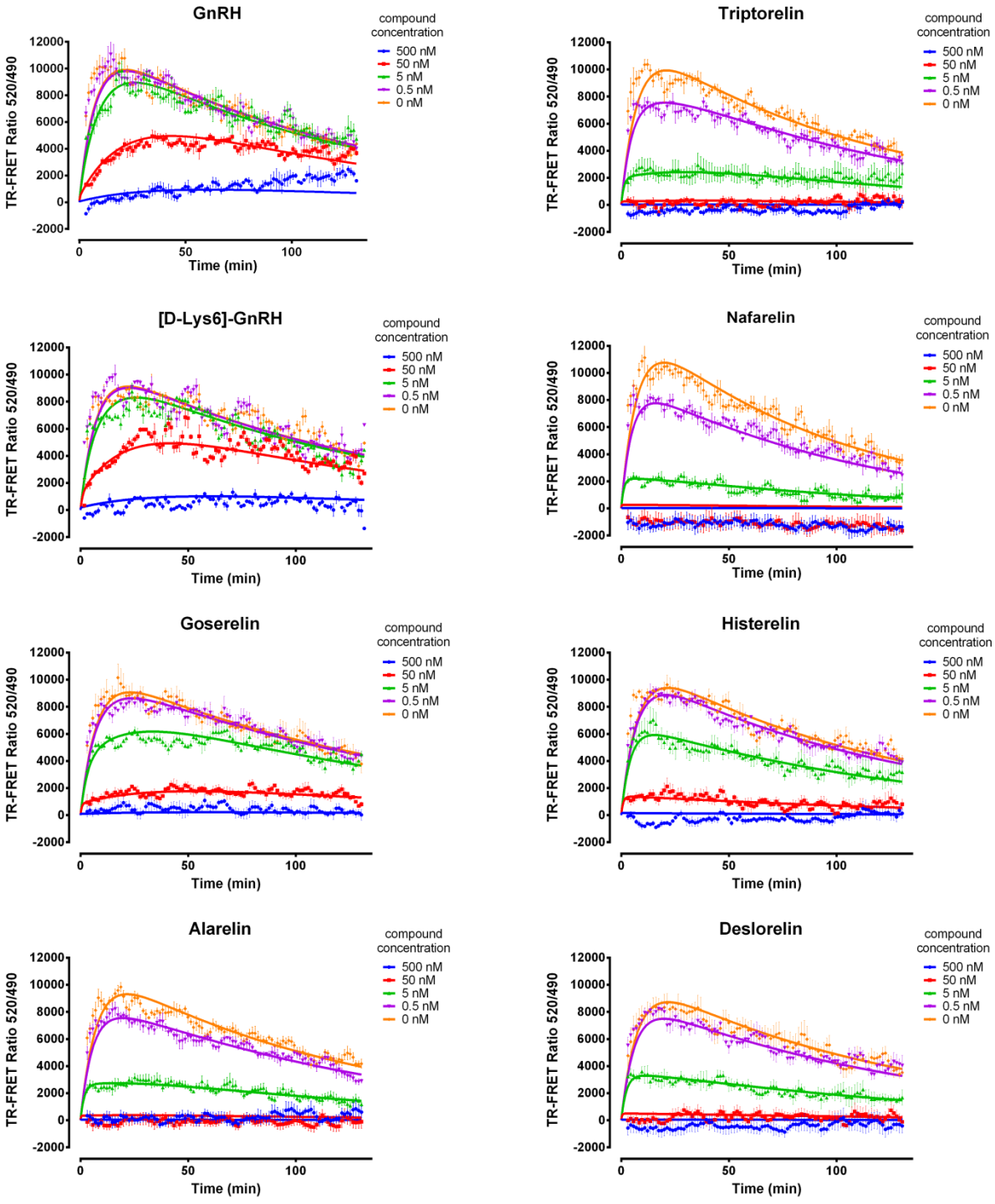

Supplementary Figure 3. kPCA traces of the GnRH peptide agonists analyzed. Four concentrations (0.5, 5, 50 and 500 nM) were examined. Representative graphs from one experiment performed in duplicate.